

# Graph-Based Multimodal and Multi-view Alignment for Keystep Recognition

Julia Lee Romero<sup>1</sup>, Kyle Min<sup>2</sup>, Subarna Tripathi<sup>2</sup>, Morteza Karimzadeh<sup>1</sup>

<sup>1</sup>University of Colorado Boulder, <sup>2</sup>Intel Labs

## Abstract

Egocentric videos capture scenes from a wearer’s viewpoint, resulting in dynamic backgrounds, frequent motion, and occlusions, posing challenges to accurate keystep recognition. We propose a flexible graph-learning framework for fine-grained keystep recognition that is able to effectively leverage long-term dependencies in egocentric videos, and leverage alignment between egocentric and exocentric videos during training for improved inference on egocentric videos. Our approach consists of constructing a graph where each video clip of the egocentric video corresponds to a node. During training, we consider each clip of each exocentric video (if available) as additional nodes. We examine several strategies to define connections across these nodes and pose keystep recognition as a node classification task on the constructed graphs. We perform extensive experiments on the Ego-Exo4D dataset and show that our proposed flexible graph-based framework notably outperforms existing methods by more than 12 points in accuracy. Furthermore, the constructed graphs are sparse and compute efficient. We also present a study examining on harnessing several multimodal features, including narrations, depth, and object class labels, on a heterogeneous graph and discuss their corresponding contribution to the keystep recognition performance.

## 1. Introduction

Analyzing skilled single-person activities is emerging as an enabler for next-generation applications such as virtual assistants and human-AI collaborations [22, 24]. Among many research directions, keystep recognition has been instrumental in understanding task structure and procedural analysis from single-person activities.

Keystep recognition as a task has been benchmarked on either first-person (egocentric) videos or third-person (exocentric) videos due to the absence of paired ego-exo view videos [6]. Even when paired ego-exo views exist, in many instances, the exo view is not available at inference time, as is the case for wearable devices. However, egocentric videos present many challenges for keystep recogni-

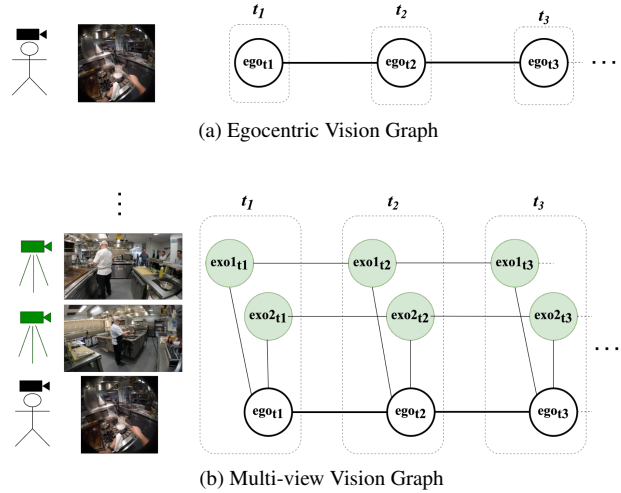


Figure 1. Graph-based representation learning for keystep recognition. Learning leverages additional exocentric views via multi-view alignment. Inference is always over the egocentric view only.

tion due to frequent movement of the viewport, changing background, and dynamic objects that move in and out of the frame. Therefore, the community has started to see renewed interest in developing keystep recognition methods that can leverage multi-view data only during training for improved performance at inference time, resulting in a collaborative effort to create a benchmark dataset [7]. We develop a compute-efficient approach for fine-grained keystep recognition on procedural egocentric videos that leverages long-term dependencies more efficiently for improved egocentric-only predictive performance while allowing for further improvement with a variable number of exocentric videos available only during training as demonstrated in Figure 1.

In this work, we focus on the the newly released Ego-Exo4D dataset [7] and the associated benchmark task challenge of fine-grained keystep recognition, which aims to improve video understanding in egocentric videos. While the task is to classify temporal action segments, or *keysteps*, in egocentric videos, multiple exocentric video takes are available during training. This dataset is complex and diverse

with videos capturing procedural actions relating to cooking, bike repair, and health in different settings and with large variations in video lengths. The keystone actions are fine-grained and many involve manipulation of the same objects in the scene. Additionally, keysteps may occur over different time scales, rendering keystone recognition a challenging task.

Fine-grained keystone recognition, which is recognizing the step a camera wearer is performing, is non-trivial and warrants addressing the inherent unique challenges associated with this task. First, keysteps in the same activity may look similar and may involve differentiating subtle differences in hand-object interactions, often in the presence of occlusions and head motion. Second, this task should leverage long-form video reasoning since the sequences of keysteps and the overall activity are correlated. Finally, this task encourages investigation into methods that can effectively learn from multi-view video data and infer from the egocentric video only to be applicable for real-world use.

To summarize, below is the list of our contributions.

- **Graph-based representation learning for long-videos:** We propose a compute-efficient, graph-based representation learning framework for modeling temporal dynamics in long-form videos. We refer to this framework as MAGLEV, Multi-view Alignment with Graph for Long and Effective Video understanding.
- **Multi-view alignment with graph:** MAGLEV fuses complimentary information from variable number of multiple views in a flexible manner by learning multi-view alignment.
- **Heterogenous graph learning using multimodal alignment:** We also present a study on how to leverage complimentary multimodal information using the MAGLEV-Hetero framework. We consider additional modalities such as detected object classes, narrations, and depth maps.
- **Extensive experiments on Ego-Exo4D:** MAGLEV notably outperforms existing egocentric methods by more than 15%, and it can leverage multi-view (egocentric and exocentric views) and multimodal alignment to improve the performance further, outperforming existing multi-view methods by more than 12%. MAGLEV emerges as a new state-of-the-art method for fine-grained keystone recognition task, all the while being memory and compute efficient.

## 2. Related Work

**Keystone Recognition** Ego-Exo4D [7] is the first dataset that provides a unique learning setup to consider large-scale paired first-person (egocentric) and third-person (exocentric) views. It also has various benchmarks, including

the task of fine-grained keystone recognition, which we focus on in this paper. An initial study of this task encompasses a diverse set of baseline approaches, such as models learned for action classification (TimesFormer [2]), video-language pre-training (EgoVLP2 [18]), view-invariant two-stage training, view-point distillation and Ego-Exo transfer [11] with an improved backbone. Using both egocentric and exocentric videos during training provides similar or even worse performance when compared to using Ego-view only in the first two baselines, indicating that a more advanced method is required to fully leverage these multi-view data.

In this work, we propose a novel framework, MAGLEV, equipped with long-form reasoning, that substantially outperforms these baselines using only egocentric view, and its performance is further improved by utilizing multi-view videos. Our method is based on the recent advancement of graph-based representations for video understanding as described below.

### Graph-based Representations for Video Understanding

A line of work [1, 19, 27] explored scene graphs for video understanding, emphasizing the effectiveness of the structured representations in understanding temporal actions and interactions within videos. It has also been shown that graph-based representations without ground-truth graph annotations can be effective for lightweight frameworks for video understanding applications, including active speaker detection [16, 17]. In comparison, graph-based representation learning for egocentric videos is a relatively nascent field. Recently, the Ego4D [6] dataset has motivated a few works focusing on egocentric videos. In [14, 15], the authors show how the graph-based representation can be leveraged for audio-video diarization in egocentric videos. The task of scene graph generation is addressed in [13] by composing information from third-person and first-person views to construct scene graphs. The work of [20] introduces a temporally evolving graph structure of the actions performed in egocentric videos and proposes a new graph generation task.

Our approach is distinguished from the literature in the sense that we formulate the problem of fine-grained keystone recognition as node classification on a graph constructed from the input egocentric videos, while leveraging the variable number of exocentric videos only during training.

## 3. Methodology

### 3.1. Problem Formulation

Ego-Exo4D’s keystone recognition task is classification on trimmed video clips [7]. At training time, we are given egocentric videos and their aligned exocentric videos, while at test time, only the egocentric videos and the trimmed clip segments are provided.

### 3.2. Multi-Layer Perceptron Baseline

Since all prior approaches operate directly on video, and our approach uses the pre-extracted omnivore features, we train and evaluate a simple multi-layer perceptron (MLP) on the Omnivore features as a baseline (in addition to comparing against the State of the Art). The MLP consists of an input layer, a hidden layer with 1056 units and ReLU activation, and an output layer.

### 3.3. Graph Architecture

We construct a graph given an input video and keystone segments within the video. Here, first, we introduce the base graph architecture and then describe each of the modifications made to the architecture for the experiments.

Given the egocentric video, we construct a temporal graph where each node corresponds to a keystone segment. Let  $G = (V, E)$  be a temporal graph where  $V$  represents the set of nodes and  $E$  represents the set of edges. Edges  $e \in E$  connect subsequent action segments, facilitating temporal information flow. Additionally, each node  $v$  has a self-loop. Let  $X$  be the set of node features  $\{x_v\}_{v \in V}$ , where  $x_v$  is the feature vector associated with the node  $v$ .

Edges may be forward, backward, and undirected. We perform experiments on edge directionality and report results in Section 4.2.3. Please refer to [17] for further details and experiments on edge directionality.

The model is trained on a node classification task, such that a keystone prediction is made for each node in the graph.

We use the pre-extracted Omnivore Swin-L vision features ( $n=1536$ ) from 32/30 second-length windows on each video [5]. Node features  $X$  in the graph are obtained by simply averaging these features for each clip.

We use the PyTorch-Geometric package [4] to implement the graphs and graph layers described in the following sections. Next, we describe the homogeneous graph structures for egocentric view only, and for egocentric+exocentric multi-view.

#### 3.3.1 Egocentric Vision Graph

In the egocentric-only graph (Figure 1a),  $G = (V, E)$ , all nodes are egocentric  $V = V_{\text{ego}}$  where  $V_{\text{ego}}$  represents the set of egocentric nodes, and all edges  $E$  are temporal,  $E = E_{\text{temp}}$ . There is one node per keystone segment and edges are drawn between subsequent nodes such that the graph is temporally ordered. In this setup, there is only one node type (vision) and one edge type (temporal).

#### 3.3.2 Multi-view Vision Graph

Building on the egocentric vision graph, we define a multi-view graph  $G' = (V', E')$ , which adds a node for each exocentric view for each keystone segment such that  $V' =$

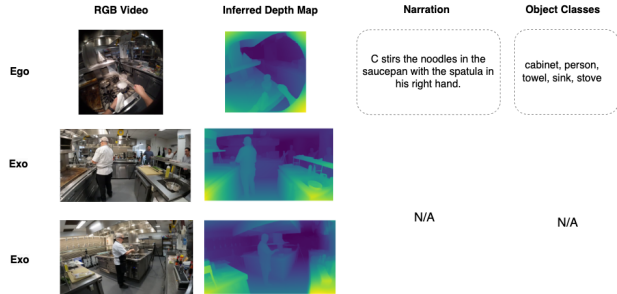


Figure 2. There are four data modalities integrated into the graph framework, depending on the experiment group. Narrations and object classes are computed only for the egocentric view, and depth maps are computed for each view. There are between three and five exocentric views per scenario.

$V_{\text{ego}} \cup V_{\text{exo}}$ , where  $V_{\text{exo}}$  represents the set of exocentric nodes. All the nodes represent the same visual features, and therefore, the graph remains homogeneous having one node type. We introduce a new edge type, cross-view edges,  $E_{\text{cross}}$ , that connect egocentric and exocentric nodes within the same temporal segment. Temporal edges,  $E_{\text{temp}}$ , connect nodes of the same view across subsequent keystone segments. Thus,  $E' = E_{\text{temp}} \cup E_{\text{cross}}$ . Refer to Figure 1b for an overview of the vision graph framework.

We construct multi-view graphs that are used to train the graph layers. During inference, we use the corresponding egocentric-only graph,  $G_{\text{inference}} = (V_{\text{ego}}, E_{\text{temp}})$ . Only egocentric nodes and temporal edges are used for node classification.

We experiment with strategies for drawing edges connecting egocentric and exocentric nodes and test different graph architectures. We examine the impacts of graph layers including edge convolutions (EdgeConv) [25], graph attention (GAT) [3], GraphSAGE operations (SAGEConv) [8], and relational graph convolution (RGCN) [21].

#### 3.3.3 Heterogeneous Graph for Multimodal Data

Building on the base egocentric and multi-view vision graph setups, we further extend our graph construction to heterogeneous graphs incorporating multiple modalities. Specifically, we construct heterogeneous graphs for three different combinations of modalities: vision+depth, vision+text, and vision+text+depth.

In all graphs, we use the Omnivore Swin-L features as the vision features. Next, we describe our methods for generating depth and text features and constructing the heterogeneous graph for each combination.

**Vision + Depth Graph** We hypothesize that integrating depth data can provide additional spatial information to the graph and that incorporating multi-view depth data can further strengthen multi-view learning by providing a more

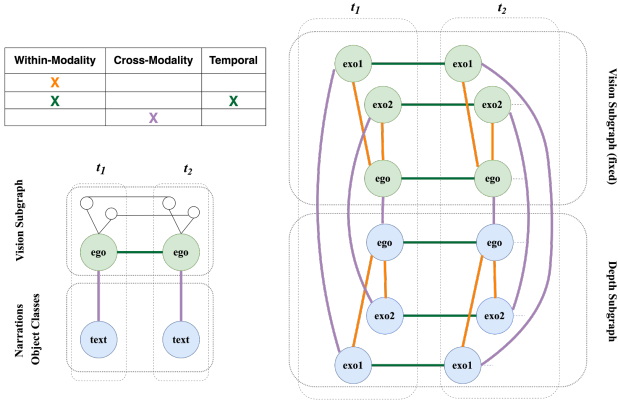


Figure 3. Illustration of the possible edge connection types within the graph framework. For narration and object class modalities, there is a single node added and connected to the ego vision node. Depth graphs can contain several edge types: within-modality edges, cross-modality, and temporal. Edges that connect matching node types share weights (e.g.,  $E_{\text{depth-vision}}$ ,  $E_{\text{depth-depth}}$ ,  $E_{\text{text-vision}}$ ).

comprehensive understanding of the spatial dynamics in the scene. We utilize Depth Anything V2 [26] to generate pixel-level depth maps on each camera view (ego and exocentric). From each keystone segment and camera view, the middle frame is sampled to generate the depth features. The exocentric depth maps are center-cropped to match the egocentric dimensions of 448x448 pixels and subsequently down-scaled to 56x56 pixels, resulting in a depth feature dimension of  $n=3136$ .

In the vision+depth graphs, we begin with the base graph and add a node for each keystone segment per view, thereby doubling the number of nodes in the graph. In the egocentric setup, we begin with  $G$  and add depth nodes corresponding to the egocentric view and introduce directed edges from each depth node to the vision node within the same keystone segment.

In the multi-view setup, starting with  $G'$ , we add depth nodes for both egocentric and exocentric views. Edges are drawn between depth nodes and between depth and vision nodes. We experiment with the following types of edges:

1. Cross-depth-view edges from exocentric depth nodes to egocentric depth nodes.
2. Cross-modality and same-view edges from depth nodes to the corresponding vision nodes.
3. Temporal edges between same-view depth nodes across subsequent keystone segments.

**Vision + Text Graph** For the text modality, we explore two methods to generate text features. First, we use the recent VideoRecap [10] framework to generate text narrations for 4-second clips spanning the video length and summarize

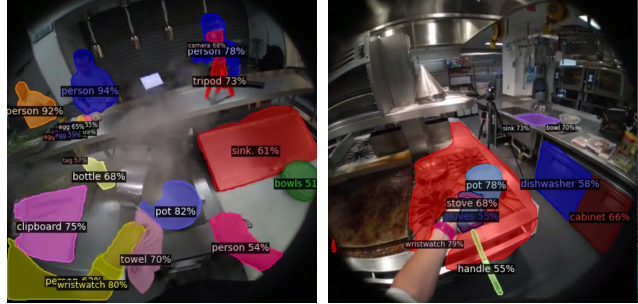


Figure 4. Detic object detection on frames.

these narrations for keystone segments. VideoRecap is pre-trained on the Ego4D dataset, and we use the off-the-shelf weights to generate segment-level captions.

The keystone actions are fine-grained and we noticed the model having trouble distinguishing between similar actions involving different ingredients, for example cut scallion, cut spring onions, cut cabbage, and cut celery. Incorporating object detection into the framework may alleviate this type of classification error, so we utilized the Detic object detector [28] to annotate the presence of certain objects using the egocentric view only. Given a video, we ran Detic on every 25th frames with a custom vocabulary containing all nouns detected in the keystone action class texts provided with Ego-Exo4D, resulting in 819 objects in the vocabulary.

We extracted CLIP features from both types of text inputs. We define a new text node type,  $v_t$ , and for each keystone segment in both the egocentric and multi-view graphs, we add a text node. Formally, let  $V_t$  represent the set of text nodes, and we augment the graph  $G = (V, E)$  to  $G_{\text{text}} = (V \cup V_t, E \cup E_t)$ , where  $E_t$  represents the new edges connecting text nodes to their corresponding vision nodes. This ensures that each keystone segment vision node  $v \in V$  is connected to its corresponding text node in  $V_t$  via the edge set  $E_t$ .

**Vision + Text + Depth Graph** Finally we introduce a graph setup that incorporates vision, text, and depth features. We construct the graph  $G_{\text{text+depth}} = (V \cup V_t \cup V_d, E \cup E_t \cup E_d)$ , where  $E_d$  represents the edges connecting depth nodes to their corresponding vision nodes. This graph setup combines all the properties of the previous configurations, ensuring that each keystone segment vision node  $v \in V$  is connected to its corresponding text node in  $V_t$  and depth node in  $V_d$ . Edges can be drawn between depth nodes, between depth and vision nodes, and between text and vision nodes.

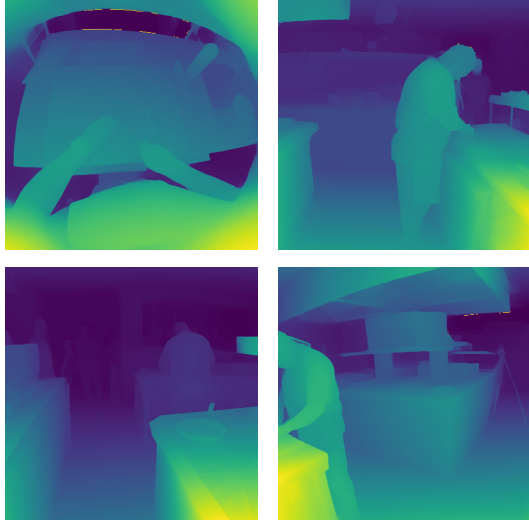


Figure 5. Corresponding egocentric and exocentric frame depth maps.

## 4. Experiments

### 4.1. Experimental Setup

#### 4.1.1 Dataset

We use the full Ego-Exo4D dataset for the fine-grained keystep recognition task [7] in this work. This includes 1088 video takes lasting 87 hours in total, with an average of 4.8 minutes per video. There are 76,057 keystep segments in total, summing the number of egocentric and exocentric segments, and these average 11.95 seconds. There are 60,639 segments in the training/validation set and 15,418 in the test set, captured from 14 cooking recipes, two health procedures, and four bike repair tasks. The dataset contains 664 unique keystep classes, but the task specifies removing long-tailed classes that occur less than 20 times, and there are 289 classes after filtering these out.

In our graph setup, the number of graphs in the ego-only and the multi-view setup are equal since all available views are used in one graph. Each node in the graph is used during training, such the multi-view setup has more samples than the ego-only setup.

#### 4.1.2 Training and Evaluation

For training and evaluation, we employ cross-validation and split the graphs into five splits. We report the validation performance as the average accuracy on the five splits. The framework is trained on each set of 4 splits and evaluated on the remaining split. In accordance with the Ego-Exo4D keystep recognition task definition, we evaluate top-1 keystep recognition accuracy and also report an F1 score at the threshold of 0.1 (F1@0.1). Note that our validation

set differs from Ego-Exo4D’s defined validation set, so the reported validation scores are not on the same data. However, the test score is directly comparable, since it is generated by the hosted evaluation server for the benchmark challenge.

We experiment with different batch sizes. The graphs vary in size, so each batch contains a variable number of training samples. The batch size indicates the number of graphs in the batch, rather than the number of training samples (nodes). We set up the baseline MLP batch sampling process to mimic the graph sampling process, so they are directly comparable. Unless otherwise specified, we use a batch size of 32 in our experiments, as determined by our batch size ablation study, and we trained for up to 60 epochs, selecting the model with the lowest validation loss. Our implementation is based on an open-sourced library: <https://github.com/IntelLabs/GraVi-T>.

## 4.2. Experimental Results

Method	Train data	Val	Test
TimeSFormer [2] (K600)	ego	35.25	35.24
TimeSFormer [2] (K600)	ego, exo	32.67	29.84
EgoVLPv2 [18] (Ego4D)	ego	36.89	37.51
EgoVLPv2 [18] (Ego4D)	ego, exo	37.03	36.84
EgoVLPv2 [18] (EgoExo)	ego	37.61	37.85
EgoVLPv2 [18] (EgoExo)	ego, exo	38.21	38.69
VI Encoder [23] (EgoExo)	ego, exo	40.23	40.61
Viewpoint Distillation [9]	ego, exo	37.79	38.10
Ego-Exo Transfer MAE [12]	ego, exo	36.71	35.57
MLP baseline	ego	25.82	-
<b>MAGLEV</b>	ego	54.69	52.36
<b>MAGLEV</b>	ego, exo	<u>56.74</u>	<u>53.08</u>
<b>MAGLEV-Hetero</b>	ego	<b>56.99</b>	<b>53.65</b>
<b>MAGLEV-Hetero</b>	ego, exo	56.62	-

Table 1. Top-1 accuracy on keystep recognition. Existing methods reported in [7] in addition to our models. The MAGLEV test results were obtained by submitting to the evaluation server. MAGLEV-Hetero results are reported for the best multimodal setup which was vision + generated narrations. MLP baseline and our model use frame-level Omnivore features. We decided not to generate test server results for the MLP baseline because of its inferior validation results.

### 4.2.1 Comparison to Existing Approaches

**Performance** We report the results of prior approaches alongside MAGLEV’s best results and an MLP baseline on omnivore features in Table 1. These results demonstrate that MAGLEV improves upon prior best ego-only and ego-exo setups by substantial margins. To obtain the test results of our methods, we submitted them to the evaluation server,

which is a direct comparison to the existing approaches. The evaluation server only records the top-1 accuracy metric.

The best prior approach on ego-only training data is EgoVLPv2 (pretrained on Ego4D) which achieves 36.89% on the validation set and 37.51% on the test set. MAGLEV’s ego-only setup achieves 54.69% on validation and 52.36% on the test set, outperforming the prior best ego-only setup by 15.02 points in accuracy on test data.

The best overall performing prior method is the View-Invariant (VI) encoder trained on ego-exo pairs which achieves 40.23% and 40.61% on the validation and test sets, while MAGLEV’s multi-view setup achieves 56.74% and 53.08% accuracy, respectively. MAGLEV outperforms the VI encoder by 12.47 test accuracy points.

**Ability to Leverage Multiple Views** One goal of the keystep recognition task is to leverage paired ego-exo training data. Many of the existing approaches suffer a drop in performance when exo views are added to the training. For example, TimeSFormer (K600) accuracy drops from 35.24% on ego-only to 29.84% with ego-exo pairs on the test set, despite being pre-trained on a large exocentric action dataset. The EgoVLPv2 model pre-trained on the Ego-Exo4D data and trained on ego-exo pairs yields an improvement from 36.69% to 37.85%. Similarly, MAGLEV exhibits a performance gain from 52.36% to 53.08% from the ego-only to the multi-view setup. Our results demonstrate that MAGLEV is able to effectively leverage multi-view information. Similar to few prior approaches that exhibit performance gains with ego-exo views, MAGLEV’s performance gain is small.

An additional note is that some methods use two pairs of ego-exo views rather than multi-view. VI Encoder uses all combinations of ego-exo two-paired views, using each available exo view as an individual sample, while Viewpoint Distillation and MAGLEV utilize all ego-exo views simultaneously in a multi-view setup. Employing each ego-exo pair as separate samples increases the size of the training dataset which may be beneficial, yet some of the exocentric views may be poor quality and capture little information about the scene which could impair learning.

Both tactics yield similar performance gains compared to using only egocentric views. Whether to use ego-exo two-pairs or multi-view depends on the flexibility of the framework; for example, VI Encoder is only able to handle paired data, while Viewpoint Distillation and MAGLEV are able to handle both. It remains an open question whether one tactic holds a significant advantage over the other.

**Model Efficiency** MAGLEV is a lightweight and compute-efficient framework. MAGLEV can be efficiently trained from randomly initialized weights in a single phase, given any frame-level visual features as initial node embeddings, eliminating the need for resource-intensive pre-

Model	Model Size (MB)
MAGLEV only	91
MAGLEV Heterogeneous only	173
MAGLEV + Omnivore Swin-L	539
TimeSFormer	929
EgoVLPv2	4300

Table 2. Comparison of model sizes.

training steps. In our experiments, we utilized frame-level Omnivore features that are provided along side the Ego-Exo4D dataset. This not only simplifies the training pipeline but also significantly reduces the computational resources and time required to achieve competitive performance.

Another key distinction is that MAGLEV uses pre-extracted features, specifically the Omnivore Swin-L features, as these were provided by Ego-Exo4D. Existing methods did not use Omnivore features, which motivated us to evaluate an MLP baseline using the provided Omnivore Swin-L features reported in Table 1. By utilizing pre-extracted features, MAGLEV significantly reduces the computational burden typically associated with processing high-dimensional video data. This not only accelerates the training and development process but also lowers hardware requirements.

Table 2 indicates the computational load of various methods. We utilize a single NVIDIA RTX A6000 GPU, which has 50GB RAM for the entire training and evaluation process, including graph generation. The memory requirements scale with the number of segments in the video, since there is a node for each segment. The generated graphs for the ego-only setup range in memory from 8.7KB to 968KB, while the generated graphs for the multi-view setup 33KB to 4.6MB. The size of each multi-view graph scales with the number of exocentric views available. With our hardware and a batch size of 32, training the ego-only setup takes 9.8 minutes, and the multi-view graph takes 16.2 minutes. The existing approaches were trained on 4 NVIDIA V100 GPUs according to [7].

#### 4.2.2 Graph Architecture Experiments

Table 3 summarizes the performance of various graph architectures in both ego-only and exo+ego settings. The architecture combining EdgeConv and RGCN layers achieves the highest accuracy and F1 scores on both in both ego-only and exo+ego, achieving 56.30% and 56.25% respectively in the exo+ego setting. The combination of EdgeConv and SAGEConv also performs well, with notable improvements over simpler configurations.

Architecture			Ego Only		Exo+Ego	
Layer 1	Layer 2	Layer 3	Acc	F1@0.1	Acc	F1@0.1
EdgeConv	GAT	SAGEConv	51.95	53.27	49.17	51.11
EdgeConv	SAGEConv	-	54.69	54.67	53.82	54.88
EdgeConv	RGCN	-	<b>55.82</b>	<b>55.76</b>	<b>56.30</b>	<b>56.25</b>
RGCN	RGCN	-	53.71	53.94	55.34	55.41

Table 3. Experiments on different graph architectures. The best performance by each architecture is reported.

Graph Structure			Exo+Ego		
Temporal	Within-View	Ego-Exo	Exo-Exo	Acc	F1@0.1
		✓		53.25	54.16
	✓	✓	Fwd, Und	54.84	55.66
	✓	✓	✓	<b>55.99</b>	<b>56.33</b>
	✓	✓		55.17	55.39

Table 4. Experiments on different graph architectures. Performances of the EdgeConv, SAGEConv architecture are reported on one train/val split. ✓ indicates the presence of forward, backward, and undirected connections. Fwd=foward and Und=undirected.

### 4.2.3 Edge Connection Experiments

Connecting exo-views as well as ego-views seems to improve the performance. Only drawing exo-ego views is slightly worse. We observe this trend on the RGCN experiments as well.

The experiments on different graph architectures, as shown in Table 4, explore the impact of various edge connections in the multi-view setup. The inclusion of temporal connections within exo-views and ego-exo cross-view connections significantly improves performance, with the best results achieved when both forward and undirected connections are incorporated, resulting in an accuracy of 55.99% and an F1 score of 56.33%. All graph setups include temporal connections across ego-view as this is fundamental to the architecture. These findings highlight the importance of adding multi-directional connections for better model performance, particularly when integrating both ego and exo-centric information.

### 4.2.4 Batch Size Ablation Study

Table 5 presents the results of ablation studies on different batch sizes, demonstrating their impact on the model performance for both ego-only and multi-view setups. These results are reported for the EdgeConv-SageConv architecture, but we found that a batch size of 32 was optimal across all homogeneous and heterogeneous graph architectures in Table 3. The experiments reveal a significant variance in accuracy and F1 scores depending on the batch size. For both setups, the best accuracy and F1 are achieved with a batch size of 32. Increasing batch size up to 32 improves performance, but sizes larger than 32 do not further improve performance. We settled on a learning rate of 0.0005 for the

Batch Size	Ego Only		Exo+Ego	
	Acc	F1@0.1	Acc	F1@0.1
4	52.14	52.09	53.25	53.81
16	55.82	54.78	54.25	54.85
32	<b>56.53</b>	<b>55.67</b>	<b>56.07</b>	<b>56.89</b>
128	54.69	54.67	54.97	55.79
512	54.99	54.75	49.86	49.50

Table 5. Ablation on batch sizes. Performances of the EdgeConv, SAGEConv architecture are reported on one train/val split.

Features	Ego Only		Exo+Ego	
	Acc	F1@0.1	Acc	F1@0.1
Baseline	56.53	55.67	56.74	56.90
+Narrations	56.99	56.52	56.62	56.39
+Depth	53.99	53.45	54.65	54.45
+Object classes	55.36	56.21	54.50	54.45

Table 6. Results of multi-view alignment with different set of features with heterogenous graph. Omnivore is used for frame-level visual features in all cases. Baseline denotes the usage of only Omnivore features. We use CLIP for the features associated with narrations generated by VideoRecap. We use a Detic object detector to extract class labels.

batch size of 32. Various learning rates with fixed batch size affected performance by up to 2 points in accuracy. Overall, training was sensitive to hyperparameter values, however, we observed that these reported optimal values yielded stable training. These findings emphasize the importance of careful hyperparameter tuning to achieve the best model performance.

### 4.2.5 Multimodal Learning

**Narrations** We compare graph performance using pre-trained VideoRecap [10].

**Object Lists** We employed Detic [28] to create lists of detected objects in the egocentric view. On average, 12.2 objects ( $\pm 6.8$ ) were detected per segment, with the number of objects ranging from 0 to 54 objects.

**Depth Maps** Depth maps were computed for the central frame of each keystone segment. Unlike the narration and object list modalities, depth maps are generated per view, allowing for the establishment of cross-view edges between depth nodes. This approach is akin to the multi-view vision graph. To assess the impact of various edge connection types, we conduct ablation experiments in the following section.

We observe that adding depth modality to the vision graph increased both of the evaluation metrics. Notably, the F1 score for the ego-only view was the highest recorded in

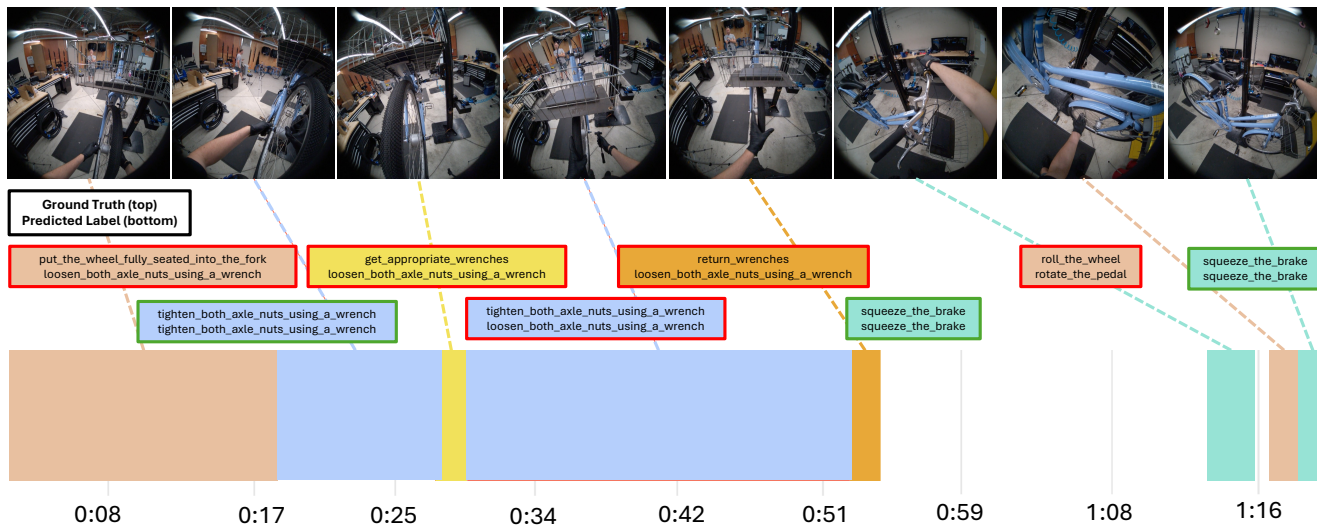


Figure 6. Qualitative results. For visualization purposes, we show one frame per segment. Each segment differently colored might have different time durations. For each pair of keystep texts, top and bottom denote ground truth label and MAGLEV predictions, respectively. The correct predictions are shown in boxes with green boundaries, whereas boxes with red boundaries denote incorrect predictions.

all ego-only experiments, while the multi-view setup’s F1 was the second highest.

### 4.3. Qualitative results

Figure 6 shows qualitative results for keystep recognition on one such egocentric video from Ego-Exo4D. Each segment are of varying duration. Segment-wise ground truth annotations and MAGLEV predicted keysteps are shown. The correct predictions are shown in boxes with green boundaries, whereas boxes with red boundaries denote incorrect predictions.

## 5. Conclusion and Discussions

We presented MAGLEV, which harnesses multi-view training strategies for fine-grained keystep recognition over long videos. We showed that our framework effectively performs on long videos, and is able to leverage complementary information from multiple views that are available only during training. We considered each clip per viewpoint as nodes in a graph and proposed several different ways of connecting those nodes. Next, we posed the keystep recognition problem as a node classification problem in the constructed graphs. Our experiments on Ego-Exo4D validation and test set show that MAGLEV notably outperforms existing methods as measured by the accuracy metric. We also conducted an extensive study on using multimodal information for heterogeneous graph learning framework, MAGLEV-Hetero. Future research will explore improved multimodal aggregation methods to further improve performance.

## References

- [1] Anurag Arnab, Chen Sun, and Cordelia Schmid. Unified graph structured models for video understanding. In *Proceedings of the IEEE/CVF International Conference on Computer Vision*, pages 8117–8126, 2021. 2
- [2] Gedas Bertasius, Heng Wang, and Lorenzo Torresani. Is space-time attention all you need for video understanding? In *Proceedings of the International Conference on Machine Learning (ICML)*, July 2021. 2, 5
- [3] Shaked Brody, Uri Alon, and Eran Yahav. How attentive are graph attention networks? *arXiv preprint arXiv:2105.14491*, 2021. 3
- [4] Matthias Fey and Jan Eric Lenssen. Fast graph representation learning with pytorch geometric. *arXiv preprint arXiv:1903.02428*, 2019. 3
- [5] Rohit Girdhar, Mannat Singh, Nikhila Ravi, Laurens van der Maaten, Armand Joulin, and Ishan Misra. Omnivore: A single model for many visual modalities. In *Proceedings of the IEEE/CVF Conference on Computer Vision and Pattern Recognition (CVPR)*, pages 16102–16112, June 2022. 3
- [6] Kristen Grauman, Andrew Westbury, Eugene Byrne, Zachary Chavis, Antonino Furnari, Rohit Girdhar, Jackson Hamburger, Hao Jiang, Miao Liu, Xingyu Liu, et al. Ego4d: Around the world in 3,000 hours of egocentric video. In *Proceedings of the IEEE/CVF Conference on Computer Vision and Pattern Recognition*, pages 18995–19012, 2022. 1, 2
- [7] Kristen Grauman, Andrew Westbury, Lorenzo Torresani, Kris Kitani, Jitendra Malik, Triantafyllos Afouras, Kumar Ashutosh, Vijay Baiyya, Siddhant Bansal, Bikram Boote, Eugene Byrne, Zach Chavis, Joya Chen, Feng Cheng, Fu-Jen Chu, Sean Crane, Avijit Dasgupta, Jing Dong, Maria Escobar, Cristhian Forigua, Abrahm Gebreselasie, Sanjay Haresh, Jing Huang, Md Mohaiminul Islam, Suyog Jain,



- Rawal Khirodkar, Devansh Kukreja, Kevin J Liang, Jia-Wei Liu, Sagnik Majumder, Yongsen Mao, Miguel Martin, Effrosyni Mavroudi, Tushar Nagarajan, Francesco Ragusa, Santhosh Kumar Ramakrishnan, Luigi Seminara, Arjun Somayazulu, Yale Song, Shan Su, Zihui Xue, Edward Zhang, Jinxu Zhang, Angela Castillo, Changan Chen, Xinzhu Fu, Ryosuke Furuta, Cristina Gonzalez, Prince Gupta, Jiabo Hu, Yifei Huang, Yiming Huang, Weslie Khoo, Anush Kumar, Robert Kuo, Sach Lakhavani, Miao Liu, Mi Luo, Zhengyi Luo, Brighid Meredith, Austin Miller, Oluwatumininu Oguntola, Xiaqing Pan, Penny Peng, Shraman Pramanick, Mery Ramazanova, Fiona Ryan, Wei Shan, Kiran Somasundaram, Chenan Song, Audrey Southerland, Masatoshi Tateno, Huiyu Wang, Yuchen Wang, Takuma Yagi, Mingfei Yan, Xitong Yang, Zecheng Yu, Shengxin Cindy Zha, Chen Zhao, Ziwei Zhao, Zhifan Zhu, Jeff Zhuo, Pablo Arbelaez, Gedas Bertasius, David Crandall, Dima Damen, Jakob Engel, Giovanni Maria Farinella, Antonino Furnari, Bernard Ghanem, Judy Hoffman, C. V. Jawahar, Richard Newcombe, Hyun Soo Park, James M. Rehg, Yoichi Sato, Manolis Savva, Jianbo Shi, Mike Zheng Shou, and Michael Wray. Ego-exo4d: Understanding skilled human activity from first- and third-person perspectives, 2024. [1](#), [2](#), [5](#), [6](#)
- [8] Will Hamilton, Zhitao Ying, and Jure Leskovec. Inductive representation learning on large graphs. *Advances in neural information processing systems*, 30, 2017. [3](#)
- [9] Geoffrey Hinton, Oriol Vinyals, and Jeff Dean. Distilling the knowledge in a neural network, 2015. [5](#)
- [10] Md Mohaiminul Islam, Ngan Ho, Xitong Yang, Tushar Nagarajan, Lorenzo Torresani, and Gedas Bertasius. Video recap: Recursive captioning of hour-long videos. In *Proceedings of the IEEE/CVF Conference on Computer Vision and Pattern Recognition*, pages 18198–18208, 2024. [4](#), [7](#)
- [11] Yanghao Li, Tushar Nagarajan, Bo Xiong, and Kristen Grauman. Ego-exo: Transferring visual representations from third-person to first-person videos. *2021 IEEE/CVF Conference on Computer Vision and Pattern Recognition (CVPR)*, pages 6939–6949, 2021. [2](#)
- [12] Yanghao Li, Tushar Nagarajan, Bo Xiong, and Kristen Grauman. Ego-exo: Transferring visual representations from third-person to first-person videos. In *CVPR*, 2021. [5](#)
- [13] Yichao Lu, Cheng Chang, Himanshu Rai, Guangwei Yu, and Maksims Volkovs. Multi-view scene graph generation in videos. In *International Challenge on Activity Recognition (ActivityNet) CVPR 2021 Workshop*, volume 3, page 2, 2021. [2](#)
- [14] Kyle Min. Intel labs at ego4d challenge 2022: A better baseline for audio-visual diarization. *arXiv preprint arXiv:2210.07764*, 2022. [2](#)
- [15] Kyle Min. Sthg: Spatial-temporal heterogeneous graph learning for advanced audio-visual diarization. *arXiv preprint arXiv:2306.10608*, 2023. [2](#)
- [16] Kyle Min, Sourya Roy, Subarna Tripathi, Tanaya Guha, and Somdeb Majumdar. Intel labs at activitynet challenge 2022: Spell for long-term active speaker detection. *The ActivityNet Large-Scale Activity Recognition Challenge*, 2022. [https://research.google.com/ava/2022/S2\\_SPELL\\_ActivityNet\\_Challenge\\_2022.pdf](https://research.google.com/ava/2022/S2_SPELL_ActivityNet_Challenge_2022.pdf). [2](#)
- [17] Kyle Min, Sourya Roy, Subarna Tripathi, Tanaya Guha, and Somdeb Majumdar. Learning long-term spatial-temporal graphs for active speaker detection. In *European Conference on Computer Vision*, pages 371–387. Springer, 2022. [2](#), [3](#)
- [18] Shraman Pramanick, Yale Song, Sayan Nag, Kevin Qinghong Lin, Hardik Shah, Mike Zheng Shou, Rama Chellappa, and Pengchuan Zhang. Egovlpv2: Egocentric video-language pre-training with fusion in the backbone, 2023. [2](#), [5](#)
- [19] Nishant Rai, Haofeng Chen, Jingwei Ji, Rishi Desai, Kazuki Kozuka, Shun Ishizaka, Ehsan Adeli, and Juan Carlos Niebles. Home action genome: Cooperative compositional action understanding. In *Proceedings of the IEEE/CVF Conference on Computer Vision and Pattern Recognition*, pages 11184–11193, 2021. [2](#)
- [20] Ivan Rodin, Antonino Furnari, Kyle Min, Subarna Tripathi, and Giovanni Maria Farinella. Action scene graphs for long-form understanding of egocentric videos. In *Proceedings of the IEEE/CVF Conference on Computer Vision and Pattern Recognition*, pages 18622–18632, 2024. [2](#)
- [21] Michael Schlichtkrull, Thomas N Kipf, Peter Bloem, Rianne Van Den Berg, Ivan Titov, and Max Welling. Modeling relational data with graph convolutional networks. In *The semantic web: 15th international conference, ESWC 2018, Heraklion, Crete, Greece, June 3–7, 2018, proceedings 15*, pages 593–607. Springer, 2018. [3](#)
- [22] F. Sener, D. Chatterjee, D. Shelepov, K. He, D. Singhania, R. Wang, and A. Yao. Assembly101: A large-scale multi-view video dataset for understanding procedural activities. *CVPR 2022*, 2022. [1](#)
- [23] Aäron van den Oord, Yazhe Li, and Oriol Vinyals. Representation learning with contrastive predictive coding. *CoRR*, abs/1807.03748, 2018. [5](#)
- [24] Xin Wang, Taein Kwon, Mahdi Rad, Bowen Pan, Ishani Chakraborty, Sean Andrist, Dan Bohus, Ashley Feniello, Bugra Tekin, Felipe Vieira Frujeri, Neel Joshi, and Marc Pollefeys. Holoassist: an egocentric human interaction dataset for interactive ai assistants in the real world. In *Proceedings of the IEEE/CVF International Conference on Computer Vision (ICCV)*, pages 20270–20281, October 2023. [1](#)
- [25] Yue Wang, Yongbin Sun, Ziwei Liu, Sanjay E Sarma, Michael M Bronstein, and Justin M Solomon. Dynamic graph cnn for learning on point clouds. *ACM Transactions on Graphics (tog)*, 38(5):1–12, 2019. [3](#)
- [26] Lihe Yang, Bingyi Kang, Zilong Huang, Zhen Zhao, Xiao-gang Xu, Jiashi Feng, and Hengshuang Zhao. Depth anything v2. *arXiv preprint arXiv:2406.09414*, 2024. [4](#)
- [27] Yu Zhao, Hao Fei, Yixin Cao, Bobo Li, Meishan Zhang, Jianguo Wei, Min Zhang, and Tat-Seng Chua. Constructing holistic spatio-temporal scene graph for video semantic role labeling. In *ACM Multimedia*, 2023. [2](#)
- [28] Xingyi Zhou, Rohit Girdhar, Armand Joulin, Philipp Krähenbühl, and Ishan Misra. Detecting twenty-thousand classes using image-level supervision. In *European Conference on Computer Vision*, pages 350–368. Springer, 2022. [4](#), [7](#)